Continuous Patterning of Nanogratings by Nanochannel-Guided Lithography on Liquid Resists

*Jong G. Ok, Hui Joon Park, Moon Kyu Kwak, Carlos A. Pina-Hernandez, Se Hyun Ahn, and L. Jay Guo**

Nanoscale grating structures can be utilized in a variety of device applications such as optics,[1] organic optoelectronics,[2] and biosensors.[3] Several techniques can be used to fabricate nanograting structures. In particular, the recently reported dynamic nanoinscribing (DNI)[4] method can create seamless large-area nanogratings on any material softer than the molds at high speed. DNI uses a slice of cleaved rigid grating mold to mechanically inscribe a polymer surface to create nanograting structures in a dynamic fashion. However, the elastic recovery of the plastically deformed solid surfaces after the release of mechanical force[5] limits the aspect ratio of the inscribed structure, especially for small period gratings. This cannot satisfy the need for many applications such as metal wire-grid polarizers,[6] where higher aspect ratios and well-defined cross-sectional profiles are desirable.[7]

To address these issues, we have developed a nanopatterning technique by adopting liquid resist materials to a high-throughput nanoinscribing process, aiming to achieve high-speed and low-cost fabrication of continuous nanograting structures for large-area optoelectronic applications. As a suitable liquid resist, we introduce UV-curable epoxy-based silsesquioxane (SSQ), which is a viscous liquid polymer that solidifies into a cross-linked high-modulus material upon UV curing without significant volume shrinkage.[8] Whereas a relatively large force is required to "inscribe" nanopatterns on a solid substrate by plastically deforming the material, a liquid resist can readily "infiltrate" the openings in the mold grating upon contact under slight mechanical force. These nanochannel-guided liquid streaks are continuously extruded from the contact region as the mold translates along the surface, enabling continuous formation of nanograting patterns without elastic recovery. To ensure the success of the nanopatterning process by this nanochannel-guided lithography (NCL), the substrate material should have non-wetting properties with respect to the liquid resist used in the process. The shallow but plastically deformed groove features on the substrate along with its non-wetting characteristics prevent the immediate reflow of the as-formed liquid nanograting structures until the pattern is fully cured by UV light.

The setup for the NCL process is schematically shown in **Figure 1**a. First, the edge of a rigid grating mold makes contact with a UV-curable liquid resist coated on a polymer substrate (i.e., perfluoroalkoxy (PFA) or polyethylene terephthalate (PET)). The grating mold is inclined at an angle of ≈15° with respect to the moving substrate and the contact force is about 5 N. The contact point can be maintained at ambient or elevated temperature, controlled by localized heating by using a conductive heater attached to the backside of the mold. The heating is used to adjust the viscosity of the liquid resist for optimal filling of the nanochannel features on the mold within the processing time. The polymer substrate is placed on a silicone rubber film, which prevents the substrate from slipping during the process and ensures conformal contact to the mold edge with the support of a multiaxial tilting stage. As the substrate is moved at a controlled speed with respective to the mold, the liquid resist material on top of the substrate is extruded from the end of the nanochannels on the mold, as illustrated in Figure 1d. A UV light placed in front of the mold promptly cures the liquid resist to form the nanogratings with a well-retained profile. Such a continuous process produces a seamless nanograting in cured liquid resist material. The mold-substrate contacting angle, θ, can be chosen between ≈10° to 35° for reliable processing; if θ is too small, it may induce excess liquid resist to infiltrate the mold openings by capillary action before entering the contact region. On the other hand, if θ becomes too large, the effective mold opening depth, $d(\cos\theta)$ where d is the original mold opening depth, becomes smaller, which can restrict liquid infiltration along the nanochannels on contact.

The key advantage of the NCL process is that it can produce nanograting structures in a UV curable liquid resist with higher aspect-ratio profiles than the ones inscribed on the solid plastic surface by the DNI process. This is demonstrated by comparing the 200 nm period grating patterned on a SSQ-coated PFA surface by NCL with the grating formed on the solid PFA by DNI, as shown in Figure 1e, f. Similar results were observed in gratings of different periods (e.g., 700 nm) and substrate materials (e.g., PET), as can be found in Figure S1 (Supporting Information). For the normal DNI patterning on solids, the plastic deformation by mechanical inscription that forms the nanograting is inherently limited by the elastic

J. G. Ok, Dr. S. H. Ahn[+]
Department of Mechanical Engineering
University of Michigan
Ann Arbor, MI 48109, USA
H. J. Park, Dr. C. A. Pina-Hernandez, Prof. L. J. Guo
Macromolecular Science and Engineering
University of Michigan
Ann Arbor, MI 48109, USA
E-mail: guo@umich.edu
Dr. M. K. Kwak, Prof. L. J. Guo
Department of Electrical Engineering and Computer Science
University of Michigan
Ann Arbor, MI 48109, USA
[+] Present address: Molecular Imprints, Inc., Austin, TX 78758, USA

DOI: 10.1002/adma.201102199

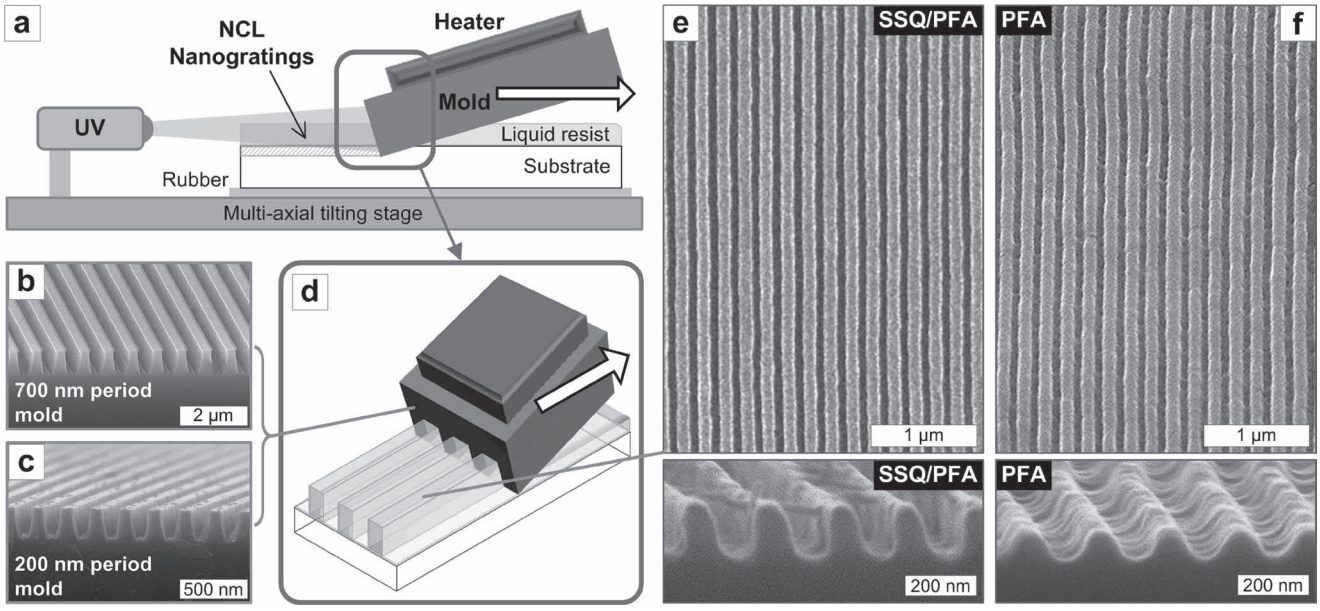

Figure 1. a) Schematics of the NCL process where the liquid resist is extruded from the nanochannels on the grating mode and promptly cured by UV light to retain the profile. A slice of the SiO_2/Si grating molds with a period of either b) 700 nm or c) 200 nm is used under ambient or heated conditions, and the liquid SSQ resist is coated on a polymer substrate (e.g., PFA or PET). An enlarged perspective view of the process (d) illustrates that the liquid lines are extruded from the openings of the mold grating in the contact region. Scanning electron microscopy (SEM) images of 200 nm period nanogratings formed on the PFA substrates at 80 °C e) with and f) without a liquid SSQ coating. The insets are the counterprofiles of each grating structure, showing that the aspect ratio of resulting nanogratings can be significantly improved by the use of SSQ layer.

recovery process. This effect hampers a reliable patterning of nanograting of smaller periods (e.g., 200 nm period) even under a very large mechanical load. In comparison, in the new NCL process, the liquid resist material can be readily filled into the nanochannels on the SiO_2/Si grating mold due to viscous flow, similar to the polymer flow process in nanoimprint lithography (NIL).[9] Excessive liquid is continuously swept away by the mold until the process terminates, which is confirmed by the experiments where the same nanograting structures are obtained despite different thicknesses of the initial SSQ resist. The final pattern appears to have slightly rounded corners due to the reflow of the as-patterned polymer liquid grating before it is fully cured, similar to the previous reports.[10] However, the as-extruded liquid streaks on the underlying surface can mostly sustain the structures without significant immediate reflow by the control of wetting properties, as will be explained.

In NCL, the liquid–solid interaction plays a critical role in determining the final profile of the nanostructures. This is because the as-formed liquid SSQ grating extruded from the nanochannel should be able to maintain its profile rather than immediate reflow before it is cured, which is directly related to the wetting property of the solid surface. Interestingly, we found that the solid substrate surface underneath the liquid SSQ layer appears to be simultaneously inscribed during the process (see Figure S2, Supporting Information). The inscribed profile on the PFA substrate is more pronounced than that of PET and the SSQ grating has a faithfully replicated profile on PFA but not on the PET substrate. We believe that the nanograting formation in the NCL process is dictated by two main factors: 1) the wetting characteristics of liquid SSQ on the solid surfaces and 2) the deformation characteristics of the solid surface. Therefore both the surface energy and elastic moduli of the solid substrate are important in this process.

Figure 2 compares the nanograting formation characteristics on solid materials (i.e., PFA and PET) with different elastic modulus. SSQ liquid resist also has different wetting behaviors on the two substrates due to the different surface energies of the two substrates. The contact angles of a liquid SSQ droplet on the flat PFA and PET surfaces at room temperature were 67.9° and 20.1°, respectively (Figure 2a1,b1). The large contact angle and the resultant non-wetting behavior of liquid SSQ on PFA will stabilize the as-formed liquid grating against reflow, allowing time for it to be cured and solidified (Figure 2a). In fact, it was observed that the grating profile remains almost static regardless of the UV curing time, confirming the self-stabilization of the as-extruded liquid lines from the nanochannels on the mold on PFA. In contrast, the small contact angle between liquid SSQ on PET dictates a good wetting behavior of the SSQ on PET that results in quick reflow of the as-formed nanograting structure (Figure 2b). One should also take into account that during the NCL process the underlying PFA surface, which has a smaller modulus ($E \approx 0.5$ GPa), is deformed more than PET ($E \approx 3$ GPa). Thus, as schematically shown in Figure 2a2, the as-formed liquid SSQ grating sitting on top of the inscribed PFA grating benefits from the large contact angle at SSQ/PFA interfaces and maintains a vertical profile, which is essential to obtain high-aspect-ratio nanograting structures. On the other hand, the shallow profile in PET due to its high modulus and the low contact angle of SSQ cannot efficiently prevent the lateral reflow of the liquid resist pattern before it is fully cured.

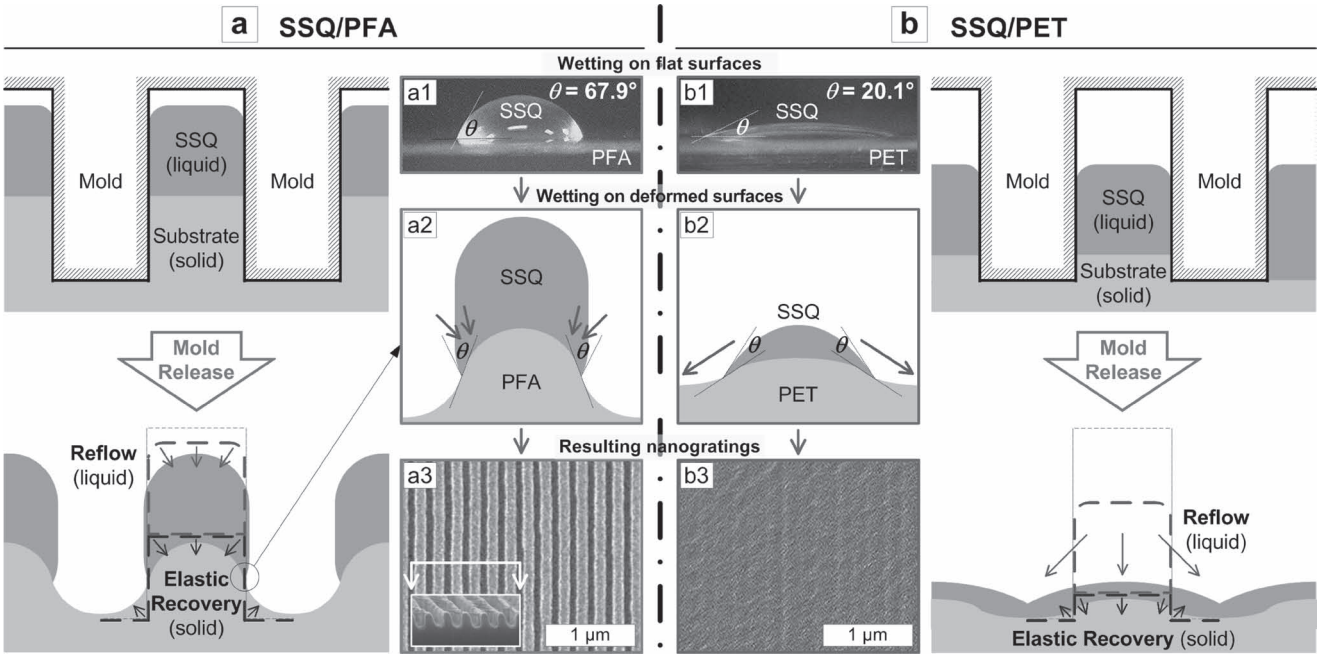

Figure 2. Diagrams of nanograting formations by the NCL process on SSQ-coated a) PFA and b) PET substrates. At contact, liquid resist is filled into the nanochannels on the mold and solid substrate is plastically inscribed by the sharp edge of the grating mold. The inscribed solid surface undergoes elastic recovery while the as-formed liquid experiences reflow depending on its wettability on the solid surface. Final grating geometry is determined by the cooperative effect of liquid wetting and substrate topography. The contact angle of SSQ droplets is much larger on PFA than on PET (a1,b1). Meanwhile, PFA is deformed more than PET due to its smaller modulus, which helps to maintain a vertical profile of the SSQ ridges on top. This is depicted in (a2) and (b2) where the subsequent reflow directions are marked with arrows. The SSQ reflow on PFA is effectively restricted by the local contact with SSQ-repellant PFA grooves, whereas the as-formed liquid SSQ lines on the PET surface shortly collapse due to the better wettability on PET along with the insufficient local deformation of the PET surface. Accordingly, the resulting nanogratings processed at 80 °C (a3,b3) show that more faithful, higher-aspect-ratio nanogratings can be created on the SSQ-coated PFA surface. The inset to (a3) shows the counterprofile of a cross-section.

To further verify the wetting-dependent mechanism, we modified the surface of the PET by fluorosilane coating to render it non-wetting to SSQ. Figure S3 (Supporting Information) compares 700 nm period SSQ nanogratings formed on the normal and fluorosilane-treated PET (F-PET) substrates by NCL, which demonstrates that the pattern profiles can be tuned by different wetting conditions on the same material substrate. Here, a much larger contact angle of SSQ to the F-PET prevents the wetting-induced reflow of liquid SSQ and allows time for the as-formed SSQ grating to be fully cured before it is relaxed by the reflow. This may enable the fabrication of high aspect-ratio nanogratings on hard surfaces, which cannot usually form very deep patterns under normal circumstances.

Understanding the flow characteristics of the liquid SSQ material, such as viscosity, is important to determine the channel filling behavior in the NCL process prior to the UV curing. We observed that the viscosity of the liquid SSQ decreases with the increasing temperature from room temperature up to around 80 °C, as presented in **Figure 3**a. It was also confirmed that liquid SSQ behaves as a Newtonian fluid since the viscosity remains constant and shear stress increases linearly with the sweeping shear rate (see Figure S4, Supporting Information). For a Newtonian liquid such as liquid SSQ and assuming laminar flow, the velocity, u, at which a mold channel is filled is proportional to $\tau(L/\mu)$,[11] where τ is shear stress, L is the channel width, and μ is the viscosity of the SSQ liquid material. This is consistent with the cavity filling time in regular NIL process.[12] In NCL, this relationship suggests that for the same applied pressure, and given a similar process speed, a grating pattern with a greater depth can be obtained for a lower viscosity SSQ due to

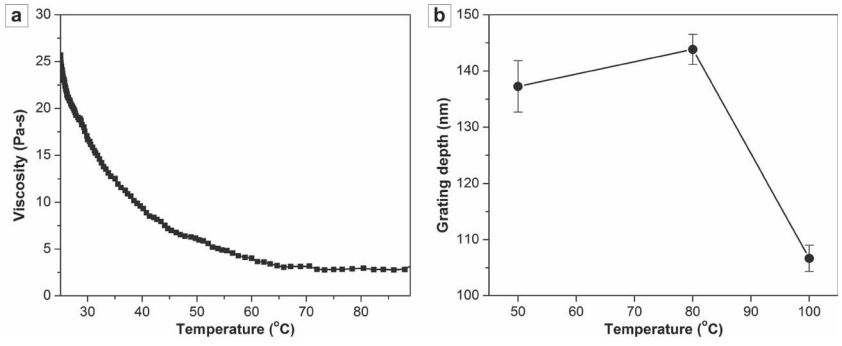

Figure 3. a) Viscosity of liquid SSQ as a function of temperature. The SSQ viscosity decreases as the temperature increases up to ≈80–90 °C. SSQ starts to cure beyond ≈90 °C, causing an increase in viscosity. b) The grating depths measured from the counterprofiles of 200 nm period nanogratings formed on SSQ-coated PFA substrates at different temperatures. The values are averaged over three different positions for each case.

a more complete filling of the nanochannels by the liquid SSQ, which can be achieved by a higher processing temperature (Figure 3b). The pattern depth becomes smaller at 100 °C than at 80 °C because the heat causes partial curing of the SSQ resist and therefore an increase in SSQ viscosity. A similar trend is observed when using PET as substrates, as shown in Figure S5 (Supporting Information).

We have demonstrated that faithful nanogratings can be fabricated by NCL with the feature size as small as 100 nm. We believe this resolution may be further scaled down by controlling the process parameters as well as selecting resist and substrate materials showing larger contact angle. Topographies on the underlying solid substrates created by mechanical inscription during NCL help the the as-extruded liquid patterns maintain a more vertical profile and therefore sustain the shape of the liquid walls while it is being cured. In our previous work on DNI, we have observed that it becomes more challenging to inscribe grooves on solids as the feature size decreases, which can be a limiting factor for the minimum feature size in the NCL process. A systematic study on this nanoscale mechanical inscription of various solids is currently in progress to extend the processability of NCL down to smaller scales. Since a processing force can be controlled to be very small, mold wear caused by continuous contacting can be significantly reduced to enhance process durability.

In conclusion, we have developed a novel technique to fabricate continuous high-aspect-ratio nanograting structures down to the sub-100 nm scale by NCL using liquid resists. The procedure of NCL process can be summarized as following: 1) A slice of grating molds, typically heated, contacts a liquid-coated substrate at an angle. 2) At mold–substrate contact, the liquid layer (SSQ) infiltrates the nanochannels on the mold, while the edge of the mold simultaneously inscribes the plastic substrate to form shallow grooves. 3) As NCL proceeds, the liquid SSQ grating is extruded from the nanochannels. 4) The nonwetting behavior of the liquid resist against the topographically deformed plastic substrate prevents the immediate reflow of the liquid grating pattern, allowing time for it to be fully cured and to become solid nanogratings. Since the UV cured resist forms discrete lines on top of the polymer substrate that has inscribed slightly, the NCL process can be regarded as a residual layer-free process. Therefore the typical process employed in NIL to remove the residual layer by anisotropic etching is unnecessary. The final geometry of liquid gratings can be tailored by the processing temperatures as well as the surface characteristics of the underlying solid substrate. Such a "direct-write" NCL patterning of liquid resists is a gentler process than the previous DNI technique and result in much more faithful pattern replication, especially for small period and high aspect ratio structures. This new technique may open a way to mass-produce large-area, high-quality nanogratings at low cost. Such nanogratings can be utilized in a variety of applications, including metal wire-grid polarizers and plasmonic color filters.[13]

Experimental Section

Preparations of Molds and Substrates: The grating molds were fabricated by nanoimprint lithography on a thermally grown SiO_2 layer on Si substrate, and the fabrication details were reported previously.[14] For the NCL process, only a thin slice of well-cleaved SiO_2/Si grating mold was needed since the patterning process is essentially based on a line contact with the liquid resist on the polymer substrate. The cleaving direction of the mold was perpendicular to the grating pattern for optimal nanochannel formation upon cleaving. Thus, extra care was taken during the mold fabrication to align the mold grating direction to the crystal planes of Si. The fabricated mold was then cut to a rectangular shape for the ease of handling and subsequent cleaving. To form a sharp and completely flat mold edge, a small notch was first made at one of the edges parallel to grating direction by a diamond scriber (McMaster-Carr) and was then snapped. Additional cleaning was applied to remove the debris generated at cleaving, if necessary. The molds used in this study had two different grating periods: 700 and 200 nm, as shown in Figure 1b, c, respectively. To prepare the substrates, a sheet of PFA or PET was first cleaned by acetone and isopropyl alcohol (IPA) followed by nitrogen drying and was then treated by O_2 plasma (17 sccm, 80 W, 30 s) to remove residual moisture and increase the surface energy by forming –OH surface groups for the ease of resist coating. Fluorine treatment on the PET surface was performed by vapor deposition of a fluorinated surfactant, (tridecafluoro-1,1,2,2-tetrahydrooctyl)trichlorosilane (GELEST, Inc.), for 15 min at 90 °C. To coat the substrates with UV-curable liquid resist, an epoxy-based SSQ ($T^{Phenyl}_{0.4}Q_{0.1}T^{Epoxy}_{0.5}$)[8] mixed with 3 wt% photoacid generator (UV-9820, Dow Corning Corp.) was diluted with propylene glycol monomethyl ether acetate (PGMEA) to make a SSQ resist solution containing 10–20 wt% SSQ. In this study the SSQ solution was spin-casted onto the substrate sheet at 500–1000 rpm. PGMEA was then completely dried to leave a thin layer of SSQ with the thickness between 400 nm and 2 μm. Spin-casting process could be replaced by a continuous coating method in the future, such as die or microgravure coating.

NCL Processing: A well-cleaved grating mold was mounted to the heater-attached holder, which was inclined typically at an angle of 15° with respect to the substrate plane. A substrate was placed on a silicone rubber film attached to a tilting stage. By adjusting the 5-DOF tilting stage (Newport Corp.), the mold edge and the substrate surface were positioned to be parallel along the contact line. The conductive heater attached to the backside of the mold was then turned on to control the process temperature, maintained by the feedback controller (Yokogawa Corp.) throughout the process. Once the temperature was in equilibrium, the edge of a mold made contact with a substrate under a slight mechanical force (≈5 N, monitored by a flexible force sensor (Tekscan Inc.)). Then, the substrate was transferred at a controlled speed (≈0.5–2 cm s^{-1}) under a conformal contact with the mold edge, to create NCL nanograting. A UV light source (7.2 W cm^{-2}, EXFO Inc.) mounted in front of the mold at 10 cm distance promptly cured the liquid resist extruding from the end of the nanochannels on the mold within 10 s, to complete the fabrication of nanograting structures with a well-retained profile.

Characterizations: SEM imaging was performed using a Philips XL30-FEG, operating at 20–30 kV, after sputtering a thin Au film (≈2–3 nm) to avoid electron charging. To prepare the cross sections, because of the difficulty to cleanly cleave the grating samples fabricated on flexible polymers (e.g., PFA or PET), they were stamped to cleaned Si substrates using epoxysilicone,[15] as a resist, followed by UV curing and cleaving. To ensure good adhesion between epoxysilicone and Si surfaces during demolding, the Si substrates, cleaned with acetone and IPA and dried by nitrogen blow, were pretreated with O_2 plasma (17 sccm, 150 W, 120 s) and then treated with epoxy-adhesion promoters (Silquest A-187, Momentive Performance Materials). Thus, all cross-sectional views shown here reveal the counterprofiles of the patterned resist gratings. The viscosity and shear stress of liquid SSQ were measured using an ARES Rheometer (TA Instruments), monitored and recorded by a TA Orchestrator. To determine both the viscosity and shear stress at different shear rates of the liquid SSQ material, a shear rate sweep was performed at room temperature by increasing the shear rate of a pair of stainless steel disk plates (1" diameter, 0.4 mm gap) uniformly filled with liquid SSQ. Viscosity as a function of temperature was then measured by sweeping the temperature

at the fixed shear rate of 1 rad s^{-1} under identical configurations. The static contact angles of liquid SSQ were measured by a home-made contact angle analyzer with real-time imaging by gently placing an SSQ droplet (≈6 μL) on the targeted surface. The presented values were averaged over at least three measurements in each case.

Supporting Information

Supporting Information is available from the Wiley Online Library or from the author.

Acknowledgements

This work was supported by NSF Grant CMMI 1000425 and the Nissan Chemical Corp. The authors gratefully acknowledge Dr. Peng-Fei Fu for useful discussions, Dr. E. Carl McIntyre and Prof. Peter F. Green for assistance with viscosity and shear stress measurements of liquid SSQ, and Bong-Gi Kim and Prof. Jinsang Kim for use of their contact angle analyzing facilities and assistance with characterization. Electron microscopy analysis was performed in the Electron Microbeam Analysis Laboratory (EMAL), and nanofabrication was performed in the Lurie Nanofabrication Facility (LNF) at the University of Michigan.

Received: June 12, 2011
Revised: July 15, 2011
Published online: August 22, 2011

[1] M. Auslender, D. Levy, S. Hava, *Appl. Opt.* **1998**, *37*, 369.
[2] a)M. G. Kang, L. J. Guo, *Adv. Mater.* **2007**, *19*, 1391; b) H. J. Park, M. G. Kang, S. H. Ahn, L. J. Guo, *Adv. Mater.* **2010**, *22*, E247; c) M. G. Kang, T. Xu, H. J. Park, X. G. Luo, L. J. Guo, *Adv. Mater.* **2010**, *22*, 4378.
[3] X. D. Hoa, A. G. Kirk, M. Tabrizian, *Biosens. Bioelectron.* **2009**, *24*, 3043.
[4] S. H. Ahn, L. J. Guo, *Nano Lett.* **2009**, *9*, 4392.
[5] J. L. White, D. Huang, *Polym. Eng. Sci.* **1981**, *21*, 1101.
[6] J. J. Wang, F. Walters, X. M. Liu, P. Sciortino, X. G. Deng, *Appl. Phys. Lett.* **2007**, *90*, 061104; b) L. Chen, J. J. Wang, F. Walters, X. G. Deng, M. Buonanno, S. Tai, X. M. Liu, *Appl. Phys. Lett.* **2007**, *90*, 063111.
[7] S. H. Ahn, J. S. Kim, L. J. Guo, *J. Vac. Sci. Technol., B* **2007**, *25*, 2388.
[8] C. Pina-Hernandez, L. J. Guo, P. F. Fu, *ACS Nano* **2010**, *4*, 4776.
[9] L. J. Guo, *Adv. Mater.* **2007**, *19*, 495.
[10] a) C. T. Pan, C. H. Su, *Sens. Actuators, A* **2007**, *134*, 631; b) J. J. Chae, S. H. Lee, K. Y. Suh, *Adv. Funct. Mater.* **2011**, *21*, 1147.
[11] J. A. Brydson, *Flow properties of polymer melts*, Van Nostrand Reinhold Co., New York **1970**.
[12] L. J. Guo, *J. Phys. D: Appl. Phys.* **2004**, *37*, R123.
[13] a) T. Xu, Y. K. Wu, X. G. Luo, L. J. Guo, *Nat. Commun.* **2010**, *1*, 59; b) A. F. Kaplan, T. Xu, Y. K. Wu, L. J. Guo, *J. Vac. Sci. Technol., B* **2010**, *28*, C6O60.
[14] M. G. Kang, M. S. Kim, J. S. Kim, L. J. Guo, *Adv. Mater.* **2008**, *20*, 4408.
[15] X. Cheng, L. J. Guo, P. F. Fu, *Adv. Mater.* **2005**, *17*, 1419.